

Wave Energy Estimation by Using A Statistical Analysis and Wave Buoy Data near the Southern Caspian Sea

A. R. Zamani and M. A. Badri¹

Research Institute for Subsea Science and Technology, Isfahan University of Technology, Isfahan, Iran

(Received 5 January 2013; received revised form 26 September 2013; accepted 12 December 2013)

ABSTRACT

Statistical analysis was done on simultaneous wave and wind using data recorded by discus-shape wave buoy. The area is located in the southern Caspian Sea near the Anzali Port. Recorded wave data were obtained through directional spectrum wave analysis. Recorded wind direction and wind speed were obtained through the related time series as well. For 12-month measurements (May 25 2007–2008), statistical calculations were done to specify the value of nonlinear auto-correlation of wave and wind using the probability distribution function of wave characteristics and statistical analysis in various time periods. The paper also presents and analyzes the amount of wave energy for the area mentioned on the basis of available database. Analyses showed a suitable comparison between the amounts of wave energy in different seasons. As a result, the best period for the largest amount of wave energy was known. Results showed that in the research period, the mean wave and wind auto correlation were about three hours. Among the probability distribution functions, i.e Weibull, Normal, Lognormal and Rayleigh, “Weibull” had the best consistency with experimental distribution function shown in different diagrams for each season. Results also showed that the mean wave energy in the research period was about 49.88 kW/m and the maximum density of wave energy was found in February and March, 2010.

Key words: *probability distribution function; nonlinear auto-correlation; wave energy; statistical analysis; Anzali Port*

1. Introduction

Rapid industrial growth has ended up with significant increase in oil consumption, resulting in the increasing dependency on renewable energies. Sea waters and wave energy are one of the newest sources of renewable energy. Although wave energy is really costly, different studies and efforts have been addressed this kind of energy. Wave buoy plays a key role in marine industry for obtaining required data. These data consist of two groups of meteorological and oceanographic data.

In recent years, various efforts have been made to utilize wave buoys in Iranian waters. In recent researches, different kinds of technologies and their theories related to wave energy absorption have been studied (Duckers, 1994; Boake *et al.*, 2002; Kofoed *et al.*, 2006; Waters *et al.*, 2007; Falcão, 2010). Also a description of wave status in deep water in Europe has been presented by Clement *et al.* (2002). In Iran, an experimental model of wave energy absorption system was designed and manufactured, but there is no research in this field based on real recorded data. Allahyar *et al.* (2008) studied the optimum network for online marine characteristics measurement of the Iranian water. Data recorded from such networks may be used to validate meteorological and oceanographic systems and to calibrate wave models for the purposes of forecast and prediction, in addition to optimum design of

¹ Corresponding author. E-mail: malbdr@cc.iut.ac.ir

marine structures. Although measurement of wave and wind has usually provided useful data for users, few calculations have been done based on real data. Parvaresh *et al.* (2005) statistically analyzed data from a wave buoy located in the Bushehr Port. They determined the linear auto-correlation coefficient of wave and wind data and finally provided an ARMA model for predicting the relation between wave and wind. In this research, wave height character was recorded by a spherical buoy and wind time series were also recorded from the coastal station. Extreme values analysis and waves return period have been done based on waves modeling data of Iranian waters in Port and Maritime Organization for Persian Gulf, Oman Sea and Caspian Sea (PMO, 2008a, 2008b), as they have been related to wave forecasting in the years from 1992 to 2003. The base of extreme analyses is presented a mathematical model data. Lari *et al.* (2000) derived the equation of wave height regression in terms of independent variables of wind speed, wind direction and temperature difference between water and air using wave buoy data located in the Bushehr Port. A neural network has been invoked with more accuracy for determining the best mapping between wave height and other variables. Wave and wind data used in this paper are related to wave and wind simultaneous measurement using an oceanographic wave buoy. As a result, the time difference measurement of wave and wind decreases to the minimum.

This paper is organized as follows: In Section 1, an introduction and history are presented. In Section 2, measurement device, location and period of measurements are introduced. The base for wave characteristics calculations using wave buoy spectral analysis and the base of wind speed time series calculations, are explained in Section 3. Statistical analyses consist of two-dimensional wave and wind histograms, wave period and height histograms. Wave probability distribution coefficients and wave and wind nonlinear auto correlation coefficient are also presented. In the wave energy part, different diagrams are shown to give a bright view of comparison between the amounts of wave energy in different seasons. The capacity of wave energy in research area is also obtained. The results of these analyses provide a clear view of wave climate in the southern Caspian Sea.

2. Materials and Methods

2.1 Measurement Data

A wave measurement buoy located at 49°26'57"E and 37°31'14"N is considered (Fig. 1).



Fig. 1. Local position of the buoy toward the Anzali Sea Port.

The buoy is disc-shaped and can send recorded meteorological and oceanographic data to the

coastal station hourly. The recording interval is from 9/5/2007 to 18/6/2008 for about 13 months. A sample of buoy measurements including wave height, wind speed, wind gust and mean wave period (T_{m01}) is shown in Fig. 2 with a continuity except one short period. Points which are out of the specified region in the wave period diagram are referred to as errors in calculations of wave buoy.

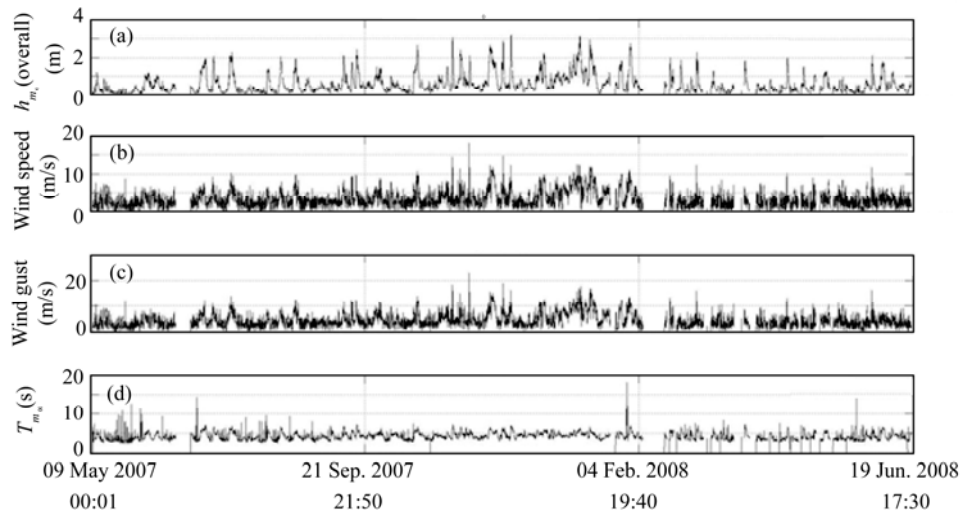


Fig. 2. Real time series measured by buoy.

2.2 Governing Equations

The hippy wave sensor which records wave data calculates wave directional spectrum by recording roll, pitch, and heave motions. The number of samples in each vertical and angular recording is 1024 with the sampling frequency of 1 Hz. Thus, the buoy records time series data to calculate wave spectrum for a time period of 20 minutes per hour and consequently sends wave integral parameters such as wave height and wave period to the coastal station. Mathematical relations used to calculate wave integral parameters from the calculated spectrum recorded by the buoy are as follows (Ochi, 1998):

$$m_n = \int f^n s(f) df ; \quad (1)$$

$$h_{m_0} = 4\sqrt{m_0} ; \quad (2)$$

$$T_{m01} = m_0 / m_1 ; \quad (3)$$

$$T_{m02} = \sqrt{m_0 / m_1} , \quad (4)$$

where f is the wave frequency, $s(f)$ is the non-directional spectrum, m_n is the n -th spectral moment, h_{m_0} is the approximation of the wave height from spectrum, T_{m01} is the mean wave period, and T_{m02} is the zero wave crossing. m_0 , m_1 and m_2 are zero, first, and second order spectral moments, respectively.

Wind speed and wind direction are measured uniformly by mechanical wind sensor which is placed at a height about 3.5 m above the sea level and records 600 samples with sampling frequency of 1 Hz. The mean measurements for a time period of 10 minutes per hour are sent as the wind speed and

the maximum measurements are sent as the wind gust with the wave data packages. The water depth of the buoy is assumed to be 20 m in this work.

3. Analysis of the Results

3.1 3D Histogram

The 3D histogram of wind speed and wave height for the whole measuring period is presented in Fig. 3 with the base of available data. The frequency of occurrence of wind and waves in the selected bins is shown in vertical axis. Similarly, the 3D histogram of the wave height and mean wave period T_{m01} is shown in Fig. 4. In the figures, the vertical axis shows the frequency of occurrence of the wave height and wave period in the selected bins.

In these figures, the frequency of occurrence is plotted for the whole measurement period. In Fig. 3 the most occurrence range is from 0 to 0.25 m. It is affected by wind speed between 2 and 3 m/s. Also, the most occurrence of wave height is from 0 to 0.25 m respectively in the interval from 2.5 to 5 s.

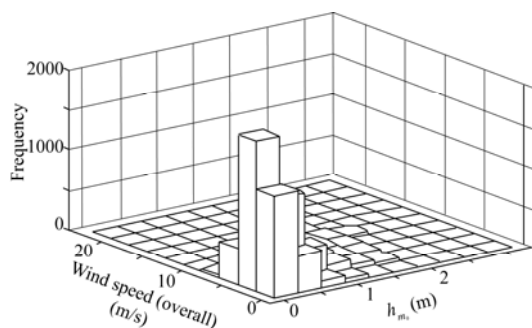


Fig. 3. Frequency of the occurrence of wind speed and wave height in the whole period of the measurement.

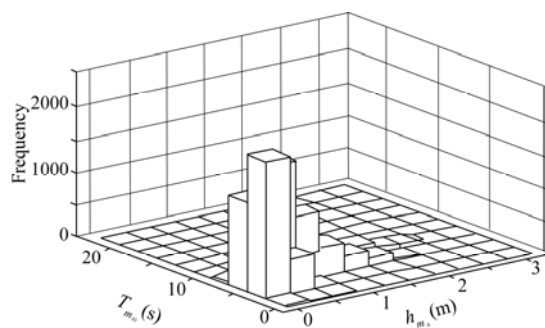


Fig. 4. Frequency of the occurrence of wave height and wave mean period T_{m01} in the whole period of the measurement.

3.2 Estimation of Density Function

Several probability distribution functions can be used to find the best fit to the real probability distribution of measured buoy data.

The experimental and mathematical probability distribution of wave occurrence is specified by real data for the following distributions (Ochi, 1998):

- Weibull distribution with statistical parameters of α and β ;
- Normal distribution with statistical parameters of μ and σ ;
- Lognormal distribution with statistical parameters of μ and σ ;
- Rayleigh distribution with statistical parameter of σ .

Fig. 5 shows the monthly probability distribution function and statistical distribution characteristics by different methods in November 2007. Experimental probability distribution function is shown in columns. It is possible to obtain probability distribution function of other months by repeating this procedure. Table 1 presents a summary distribution of parameters. Fig. 6 and Table 2 show the probability distribution functions and distribution parameters for four seasons of a year.

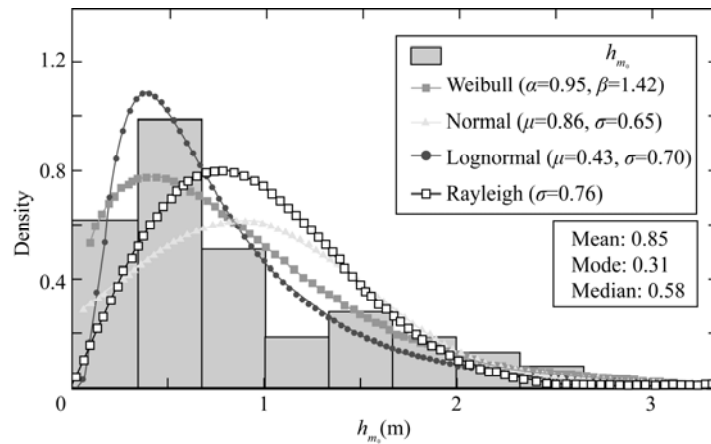


Fig. 5. Monthly probability distribution function in Nov. 2007 and statistical parameters of probability distribution.

Table 1 Selected monthly distribution parameters

Record period	Selected monthly distribution parameters						
		22/05/07	23/07/07	23/09/07	22/11/07	21/01/08	20/03/08
Weibull	α	0.36	0.42	0.61	0.95	0.66	0.46
	β	1.14	1.07	1.31	1.42	1.19	1.27
Normal	μ	0.34	0.41	0.55	0.85	0.62	0.43
	σ	0.29	0.42	0.46	0.65	0.54	0.38
Lognormal	μ	-1.54	-1.35	-0.90	-0.43	-0.88	-1.19
	σ	1.10	0.95	0.82	0.74	0.99	1.07
Rayleigh	σ	0.32	0.42	0.51	0.76	0.58	0.40

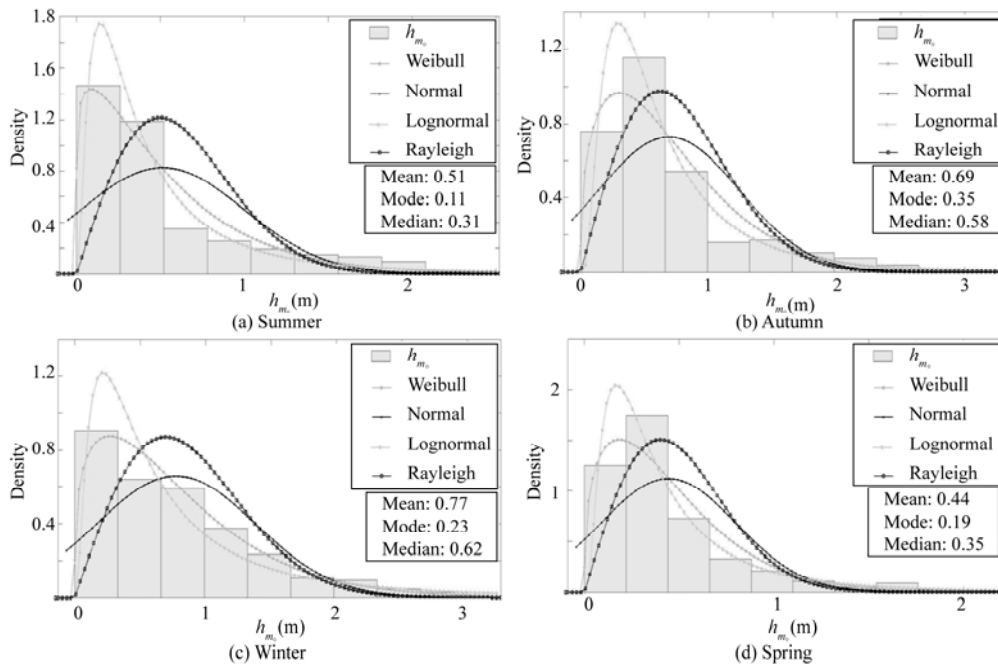


Fig. 6. Probability distribution functions for the four seasons: a) summer; b) autumn; c) winter; d) spring.

Table 2 Seasonal distribution parameters for year 2007

Season		Summer	Autumn	Winter	Spring	
Method	Weibull	α	0.54	0.76	0.84	0.49
		β	1.14	1.39	1.30	1.37
	Normal	μ	0.51	0.69	0.77	0.44
		σ	0.48	0.55	0.61	0.36
	Lognormal	μ	-1.08	-0.68	-0.61	-1.10
		σ	0.93	0.76	0.96	0.83
	Rayleigh	α	0.50	0.62	0.69	0.40

A comparison between the theoretical and the experimental probability distributions shows that the Weibull distribution function has the best overlap with local wave characteristics among different months and seasons. Some wave parameters may be obtained by the following definitions:

- Mode height (h_{mode}): wave height with the most occurrence probability.
- Median height (h_{median}): wave height in which the occurrence probability of more values is equal to the occurrence probability of fewer values.
- Mean height (h_{mean}): mean wave height.

Complete data of h_{mode} , h_{median} and h_{mean} for the measurement period are sorted in Table 3, which shows the calculated statistical wave heights for monthly, seasonal and yearly periods.

Table 3 Complete data of h_{mode} , h_{median} and h_{mean} for measurement periods

	Record period	Median (m)	Mode (m)	Mean (m)
Monthly	22/05/07–21/06/07	0.23	0.04	0.34
	22/06/07–22/07/07	0.35	0.12	0.63
	23/07/07–22/08/07	0.23	0.12	0.41
	23/08/07–22/09/07	0.39	0.31	0.54
	23/09/07–22/10/07	0.39	0.16	0.55
	23/10/07–21/11/07	0.55	0.39	0.66
	22/11/07–21/12/07	0.56	0.31	0.85
	22/12/07–20/1/08	0.94	0.7	1.05
	21/01/08–19/02/08	0.43	0.16	0.62
	20/02/08–19/03/08	0.43	0.16	0.60
	20/03/08–19/04/08	0.31	0.19	0.43
	20/04/08–20/05/08	0.31	0.16	0.41
	Seasonal	Summer 2007	0.31	0.12
Autumn 2007		0.51	0.35	0.69
Winter 2008		0.62	0.23	0.77
Spring 2007		0.35	0.19	0.51
Yearly	Whole period	0.39	0.16	0.59

3.3 Wave and Wind Nonlinear Auto-Correlation

Another statistical operation can be employed on the above data for the calculation of wave and wind nonlinear auto-correlation and the time delay between wind and wave. Auto-correlation coefficient between the two random parameters is calculated through average mutual information (AMI) method. According to Bowden *et al.* (2005), the AMI coefficient may be zero or any other

positive values. Fig. 7 shows the variation of AMI for one month. According to Fig. 7, the maximum AMI occurs in time delay of three hours. The value of time delay in the location of the maximum auto-correlation coefficient may be obtained by this procedure (see Table 4). According to Table 4, it is possible to obtain the maximum effect of wind speed on the wave height. Generally, the waves are mostly affected by local winds with mean time delay of three hours.

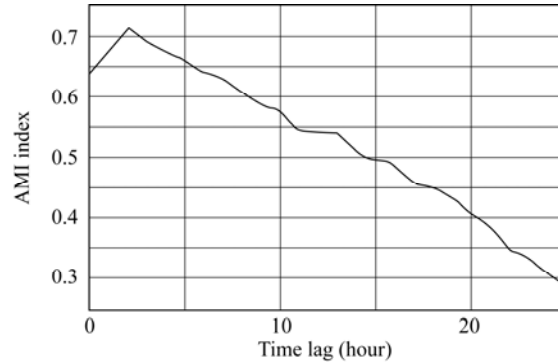


Fig. 7. Variation of AMI in Nov. 2007.

Table 4 Time delay at the location of the maximum AMI for each month

Wave and wind time delay (hour)	Record period	Wave and wind time delay (hour)	Record period
1	22/05/07–21/06/07	2	22/11/07–21/12/07
2	22/06/07–22/07/07	2	22/12/07–20/1/08
3	23/07/07–22/08/07	5	21/01/08–19/02/08
5	23/08/07–22/09/07	1	20/02/08–19/03/08
2	23/09/07–22/10/07	6	20/03/08–19/04/08
1	23/10/07–21/11/07	1	20/04/08–20/05/08
		3	Whole period

3.4 Steepness

Wave steepness is defined as:

$$s = h / \left[9.8 T_{m_{01}}^2 / (2\pi) \right], \tag{6}$$

where $T_{m_{01}}$ is the mean wave period, and h is the wave height. Fig. 8 shows the distribution of h_{m_0} and $T_{m_{01}}$ for the whole time period in different wave steepness regions ($s=0.05$ and 0.03 are plotted). This figure shows that the overall steepness of local waves is under $s=0.05$.

3.5 Time Intervals Specification

Fig. 9 presents the measured value of the significant wave height for the whole measuring period. Also, the line of $h_{m_0} = 0.5$ m is plotted in Fig. 9. Table 5 shows a summary related to Fig. 9. Similar data are presented in Table 5 for the threshold of 1 m, where n is the number of occurrence and Δt is the maximum time duration out of threshold conditions. The longest time period in which the wave height is larger than 0.5 m is presented in Fig. 10 for each month.

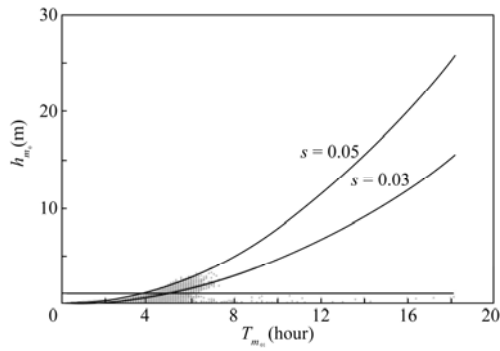


Fig. 8. Distribution diagram of h_{m_0} and T_{m_01} for the whole period and curves of $s=0.05$ and 0.03 .

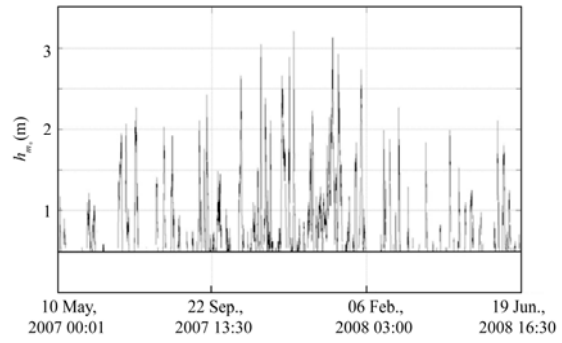


Fig. 9. Measured values of h_{m_0} larger than the threshold of 0.5 m.

Table 5 Maximum h_{m_0} of the wave height and the maximum time duration out of threshold conditions in each month

Record Period	Max. h_{m_0}	Threshold (0.5 m)	Threshold (1 m)
		Δt (hour)	Δt (hour)
22/05/07–21/06/07	1.21	68	7
22/06/07–22/07/07	2.27	90	76
23/07/07–22/08/07	2.03	67	37
23/08/07–22/09/07	2.42	103	39
23/09/07–22/10/07	2.67	74	58
23/10/07–21/11/07	3.05	115	100
22/11/07–21/12/07	3.20	191	31
22/12/07–20/01/08	3.12	217	130
21/01/08–19/02/08	1.99	54	17
20/02/08–19/03/08	2.27	41	21
20/03/08–19/04/08	1.99	43	20
20/04/08–20/05/08	2.11	67	32

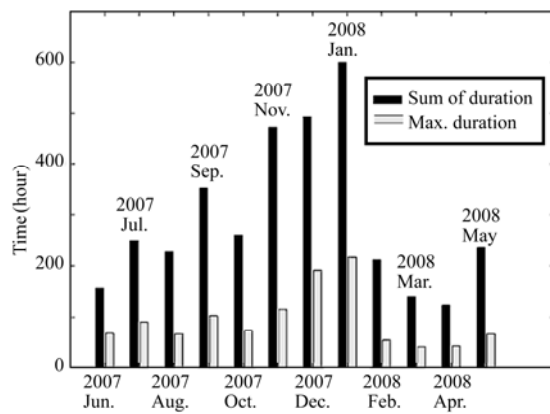


Fig. 10. Total hours and the longest time period for h_{m_0} larger than 0.5 m for each month.

3.6 Mode, Median and Mean Calculation and Maximum Daily Significant Wave Height

Highly congested data for h_{m_0} are difficult to study for the behavior of this parameter during the period. Mode, median, mean and the maximum data per day may be determined for wave probability distribution functions. Fig. 11 shows the maximum daily h_{m_0} for the whole period.

Each specified region in Fig. 11 corresponds to one month. The variation of the significant wave height for the whole period is obvious.

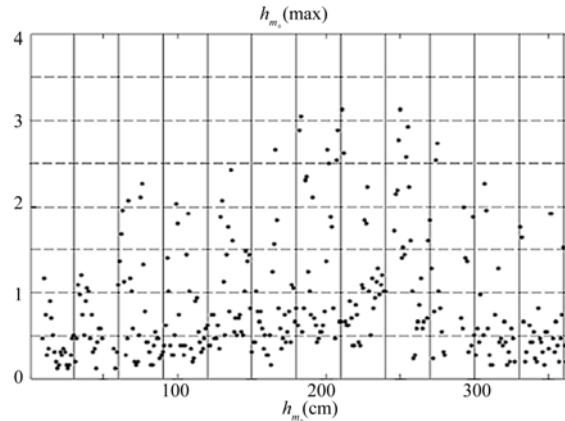


Fig. 11. Daily maximum significant wave height during the measuring period.

The relation between the maximum wave height and corresponding wind speed is analyzed in terms of the maximum daily significant wave height. Meanwhile the scatter curve during the overall period is presented. It is noticeable that the maximum wave height may be 3 m related to 10 m/s wind speed during the measuring period (Figs. 12a and 12b).

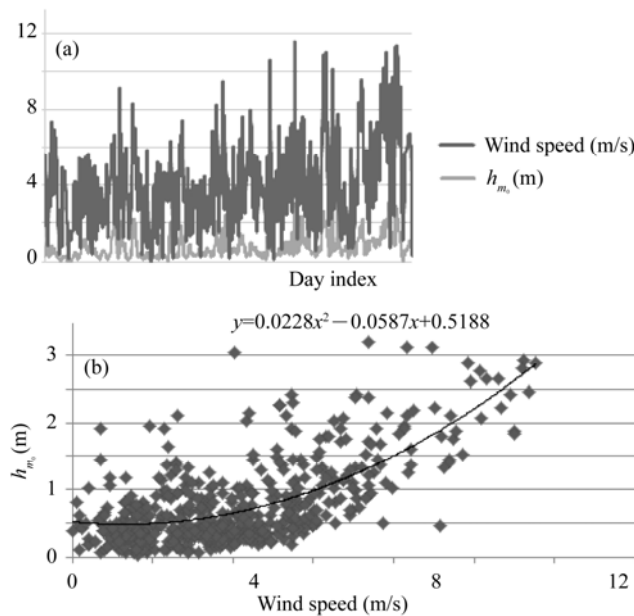


Fig. 12. Maximum daily significant wave height: a) versus wind speed at the same time; b) the scatter curve in the overall period.

4. Discussion and Results of Wave Energy Analysis

The amount of wave energy based on available databases is determined by Eq. (6):

$$p = \frac{\rho g}{64\pi} H_s^2 T_s, \quad (6)$$

where, p is the energy flux in watts per meter of crest length, $\rho = 1025 \text{ kg/m}^3$ is the density of sea water, g is the acceleration of gravity, H_s is the significant wave height, and T_s is the energy period. Statistical analysis of wave energy provides a good view of wave energy conditions in research area during specific research period (Figs. 13 and 14).

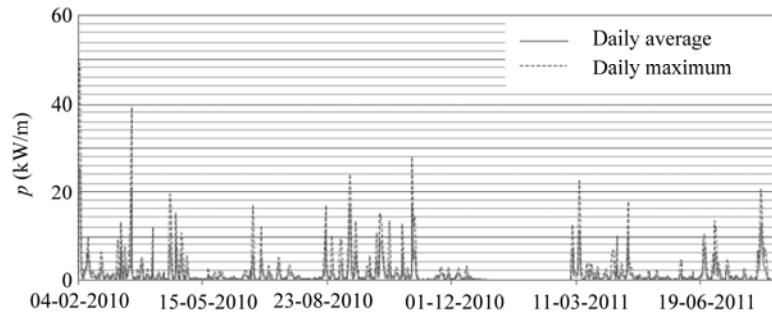


Fig. 13. Daily distribution of the maximum and the mean wave energy.

It is obvious that the maximum amount of wave energy is on Feb-10 and Mar-10, which is completely reasonable under seasonal conditions in winter. There is a discontinuity in both diagrams that are related to lack of data in the database due to the following reasons:

- (1) Wave buoy sending data problems;
- (2) Problems in receiving data from buoy in shore station;
- (3) Some mistakes in calculating values by buoy;
- (4) Sending wrong and unreasonable data to the station.

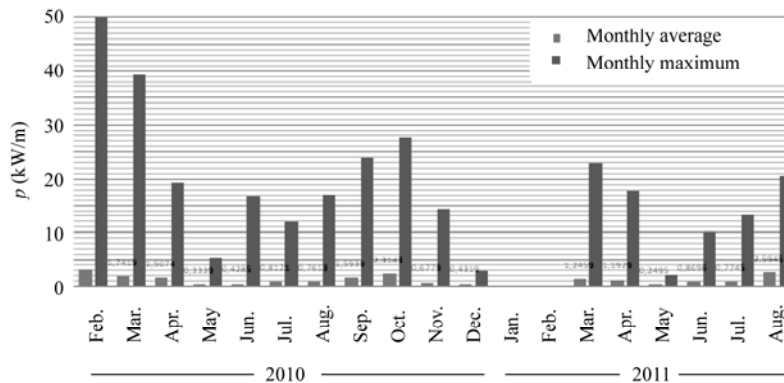


Fig. 14. Monthly distribution of the maximum and the mean wave energy.

Finally, during the whole research period, the mean value of wave energy is about 1.173 kW/m, and the maximum is about 49.88 kW/m.

In Fig. 15, the combined scatter and energy diagram can be found based on 12 months data.

Colors represent the amount of wave energy, and numerical values show the occurrence of combination of the significant wave height, wave period, and specific wave energy. Equal-energy-flux lines present the energy flux in accordance with Eq. (6). For example, it is shown that, under the conditions of the significant wave height of 0.5–1 m and the wave period of 5.5–6 s, the available wave energy is about 2 kW/m, and the number of occurrence of the waves with these conditions is 84 during the whole research period.

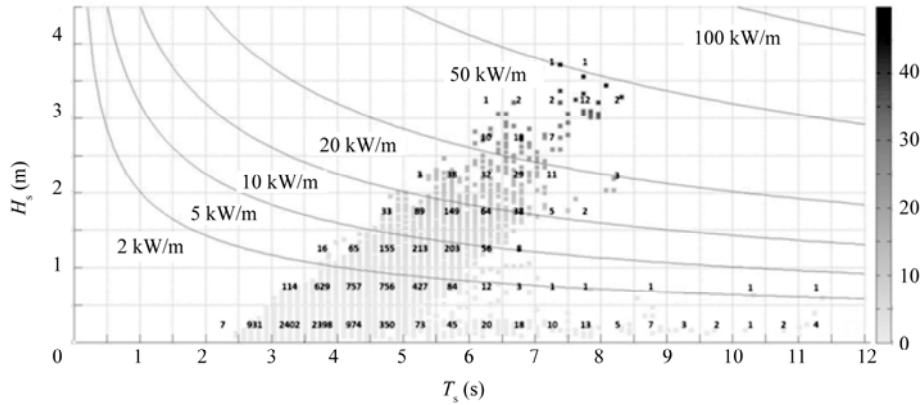


Fig. 15. Combined scatter and energy diagram during the whole period.

The maximum number of occurrence is 2402, which is related to the waves with significant wave height of 0–0.5 m, wave period of 3–3.5 s, and the capability of producing wave energy smaller than 2 kW/m. A summary of statistical results is presented in Table 6.

Table 6 Summary of statistical results

Parameter	Value
Maximum height of h_{m_0}	3.2 m
Month of maximum wave height occurrence	22/11/07–21/12/07
Median height of h_{m_0}	0.39 m
Mean height of h_{m_0}	0.57 m
Mode height of h_{m_0}	0.16 m
Mean value of wave and wind auto correlation	3 hours
Parameters of Weibull distribution function (best distribution)	$\alpha=0.63, \beta=1.20$
Maximum time duration out of threshold of 0.5 m for h_{m_0}	217 hours
Maximum time duration out of threshold of 1 m for h_{m_0}	130 hours
Maximum wave steepness	$< 5^\circ$
Most occurrence range of wave and wind	$0 < h_{m_0} < 0.25;$ $0 < \text{wind speed (m/s)} < 0.25$
Most occurrence range of wave height and wave period	$0 < h_{m_0} < 0.25; 2.5 < h_{m_0} < 5$
Maximum wave energy – whole period	49.88 kW/m
Mean wave energy – whole period	1.173 kW/m
Maximum number of occurrences	$0 < H_s < 0.5; 3 < T_s < 3.5$
Range of wave energy related to the maximum number of occurrences	$p < 2 \text{ kW/m}$

5. Conclusion

A statistical analysis based on random methods was conducted using data obtained by a discus wave measurement buoy. Data used in this research were recorded by using field measurements as a useful source for future studies towards wave analytical solution. On the other hand, wave characteristics such as wave mode, wave median, wave mean, and wave and wind auto-correlation may give a suitable view for wave and monthly wind or seasonal conditions in the southern Caspian Sea.

References

- Allahyar, M., Kebriyai, A., Dibajnia, M. and Aghajani, F., 2008. Optimum network of marine characteristics measurement of Iranian waters, *Proceedings of the 8th International Conference on Coasts, Ports and Marine Structures (ICOPMAS 2008)*, Tehran, Iran, 373–376.
- Boake, C. B., Whittaker, T. J. T., Folley, M. and Ellen, H., 2002. Overview and initial operational experience of the LIMPET wave energy plant, *Proceedings of the 12th International Offshore and Polar Engineering Conference*, Kitakyushu, Japan, **1**, 586–594.
- Bowden, G. J., Dandy, G. C. and Maier, H. R., 2005. Input determination for neural network models in water resources application, part 1–background and methodology, *J. Hydrol.*, **301**, 75–92.
- Clement, A., McCullen, P., Falcão, A., Fiorentino, A., Gardner, F., Hammarlund, K., Lemonis, G., Lewis, T., Nielsen, K., Petroncini, S., Pontes, M. T., Schild, P., Sjöström, B. O., Sørensen, H. C. and Thorp, T., 2002. Wave energy in Europe: Current status and perspectives, *Renew. Sust. Energ. Rev.*, **6**(5): 405–431.
- Duckers, L. J., 1994. Wave Energy: Crest and troughs, *Renewable Energy*, **5**(5): 1444–1452.
- Falcão, A. F. D. O., 2010. Wave energy utilization: A review of the technologies, *Renew. Sust. Energ. Rev.*, **14**(3): 899–918.
- Kofoed, J. P., Frigaard, P., Friis-Madsen, E. and Sørensen, H. C., 2006. Prototype testing of the wave energy converter wave dragon, *Renewable Energy*, **31**(2): 181–189.
- Lari, K., Poormandi, Y. A. and Mehdipour, F., 2000. Wind-generated waves forecasting based on analytical model and neural networks in Bushehr region, *Proceedings of the 4th International Conference on Coasts, Ports and Marine Structures (ICOPMAS 2000)*, Tehran, Iran, 112–119.
- Ochi, M. K., 1998. *Ocean Waves: The Stochastic Approach*, Cambridge University Press.
- Parvaresh, A., Hassanzadeh, S. and Bordbar, M., 2005. Statistical analysis of wave parameters in the north coast of the Persian Gulf, *Ann. Geophys.*, **23**(6): 2031–2038.
- Ports and Maritime Organization (PMO), 2008a. Headquarters of shores and ports engineering, Waves modeling of Iranian waters, Waves forecasting, 1992–2003, Vol. 1, Persian Gulf and Oman Sea.
- Ports and Maritime Organization (PMO), 2008b. Headquarters of shores and ports engineering, Waves modeling of Iranian waters, Waves forecasting, 1992–2003, Vol. 2, Caspian Sea.
- Waters, R., Stålberg, M., Danielsson, O., Svensson, O., Gustafsson, S., Strömstedt, E., Eriksson, M., Sundberg, J. and Leijon, M., 2007. Experimental results from sea trials of an offshore wave energy system, *Appl. Phys. Lett.*, **90**(3): 034105.